

Textile Research Journal

<http://trj.sagepub.com>

Frictional Behavior of Synthetic Yarns During Processing

Jun Lang, Sukang Zhu and Ning Pan
Textile Research Journal 2003; 73; 1071
DOI: 10.1177/004051750307301208

The online version of this article can be found at:
<http://trj.sagepub.com/cgi/content/abstract/73/12/1071>

Published by:



<http://www.sagepublications.com>

Additional services and information for *Textile Research Journal* can be found at:

Email Alerts: <http://trj.sagepub.com/cgi/alerts>

Subscriptions: <http://trj.sagepub.com/subscriptions>

Reprints: <http://www.sagepub.com/journalsReprints.nav>

Permissions: <http://www.sagepub.co.uk/journalsPermissions.nav>

Citations <http://trj.sagepub.com/cgi/content/refs/73/12/1071>

Frictional Behavior of Synthetic Yarns During Processing

JUN LANG AND SUKANG ZHU¹

Center of Physics of Fibrous Materials, Dong Hua University, Shanghai 200051, People's Republic of China

NING PAN

Division of Textiles and Clothing, Biological and Agricultural Engineering Department, University of California, Davis, California 95616, U.S.A.

ABSTRACT

The frictional behavior of synthetic yarns during various textile processes is investigated in this paper. The main advance of this work over previous research is that the deformation of the oil film lubricating the fibers is taken into consideration. The thickness of the oil film decreases due to pressure, which causes changes in the friction mechanism. To account for the transition, the effective hydrodynamic friction length during the process is defined, calculated, and discussed in this paper. The theoretical results can be used to validate and explain the findings from existing experiments made available by other researchers.

During textile processes, especially spinning and winding, textile yarns pass over guides of various types and materials, causing interfiber friction and friction between fibers and other surfaces in contact. A high frictional force will increase yarn hairiness to an unacceptable level. To reduce friction and minimize static during spinning, mineral oil is often added to lubricate synthetic fiber yarns. Cotton fibers do not need oil because the frictional behavior of cotton is quite different from synthetic fibers. Synthetic fiber friction can be influenced by a variety of factors, including speed of the yarns, guide surface roughness, film thickness, and viscosity of the lubricant. The effects of these factors will be discussed later.

Even at high speed when the friction time is extremely short, the fiber-guide contact may be treated as occurring only between an elastic body (the fiber) and a rigid one (the guide). Thus, some researchers believed the Amonton equation could not be applied to textile friction in processing [1, 2, 3, 9, 14, 20, 21], since it is fit only for purely rigid contact. Bowden and Young [5] developed an exponential relationship between the total force F due to friction and the normal force P for textiles materials.

Tremendous amounts of work [4, 9, 10, 11, 15] have been done to determine the coefficients of friction by running yarns or filaments over cylindrical surfaces. These studies concluded that the coefficient of friction was related to initial yarn tension. Therefore, the Euler equation, where the coefficient of friction is taken as a

constant, would not hold for textile materials. Based on Bowden and Young [5], Howell [9] and Lincon [11] developed Equation 1 to calculate the variations in yarn tension as the yarn passes over a cylindrical surface:

$$\frac{T_2}{T_1} = \left[1 + (1 - n)\alpha\theta \left(\frac{r}{T_1} \right)^{1-n} \right]^{1/(1-n)} \quad (1)$$

where r is the radius of the cylinder, T_1 is the initial tension, T_2 is the final tension after the yarn passes through the cylinder, and θ is the contact angle of the yarn over the cylinder.

Yet, for yarns made from synthetic fibers treated with lubricants to facilitate the process, Equation 1 is still invalid because the influence of the oil film on the yarn's frictional behavior is not taken into consideration. Hence, Hansen and Taber [8] suggested that the frictional behavior of an oil-lubricated yarn passing over a cylindrical guide could be considered analogous to that of a conventional journal bearing. Some researchers [7, 8, 13, 16] further proposed that there are three frictional mechanisms according to the frictional behavior of synthetic fiber yarns:

1. Boundary friction: the surface of the fiber and the cylindrical guide will fully contact each other.
2. Semi-boundary friction: the surface of the fiber and the cylindrical guide will contact intermittently.
3. Hydrodynamic friction: the surface of the fiber and the cylindrical guide will be separated by the oil film, characterized by significantly high frictional force.

¹ Corresponding author: zusukang@dhu.edu.cn

In hydrodynamic friction, the frictional force between the yarn and the cylindrical guide is largely determined by the characteristics of the oil. Lyne [12] conducted experiments on acetate yarns using lubricants of known viscosities. He pointed out that the velocity has the same effect as the viscosity of the lubricant on the force associated with hydrodynamic friction. By analyzing Lyne's experiments, Hansen and Taber [8] concluded that at high speed, the friction is hydrodynamic between the cylindrical guide and a yarn with an oil coating. Also, Olsen [13] summarized factors that influence hydrodynamic friction such as the velocity of the yarn, viscosity of the lubricant, yarn fineness, yarn pre-tension, surface roughness, and diameter of the guide. More completely, previous investigations concluded that the higher the velocity of the yarn, or the greater the viscosity of the lubricant, the higher the frictional force [7, 8, 18], which is related to the multiplier of velocity and viscosity. The thinner the yarn, the smaller the frictional force [17]. The higher the yarn pre-tension, the greater the friction [17]. The longer the length of the friction region, the higher the frictional force [17, 19]. At high velocity, the smoother the contact surface, the higher the friction [13, 16].

Schlatter and Demas [19] used Equation 2 to describe the frictional force for hydrodynamic friction:

$$F = \frac{\eta AV}{h} \quad (2)$$

where F is the frictional force, A is the contact area between the yarn and the guide, which is proportional to the yarn contact angle θ , V is the yarn velocity, h is the thickness of the lubricant film, and η is the viscosity of

the lubricant. From Equation 2, we can conclude that the frictional force is proportional to the area of contact, the speed, and the frictional coefficient, and inverse to the thickness of the lubricant film.

Shick [17] offered Figures 1 and 2 based on experimental data to show the relationship between the contact angle (area) and the frictional force. When the yarn speed is low, the friction is spread over a certain range as shown by the shaded areas in the figures, rather than being a single value, due to the so-called stick-slip mechanism. (The spreading converges at a critical speed, 0.01 m/min in Figure 1 and 0.5 m/min in Figure 2 roughly, into a single curve so the entire figure looks like a reversed bifurcation diagram; as interesting as it may appear, however, it is not our focus in this study.)

Nonetheless there are marked distinctions between the two figures. In Figure 1, once the spreading converges, a further increase of speed leads to a drastic climb in the friction, whereas in Figure 2, a further increase of speed has little effect on friction. Consequently, the friction in Figure 1 is significantly greater than that in Figure 2.

Although Shick thought that both experimental results were in agreement with Equation 2 at high speeds beyond the stick-slip stage, these drastic differences at the same yarn speed reveal the possibility of changes in frictional mechanisms.

We would like to argue that when the yarn speed is given and remains constant, both the contact area and the frictional coefficient are not likely to fluctuate very much. The only parameter left is the thickness of the lubricant, which may be responsible for the different behavior in Figures 1 and 2.

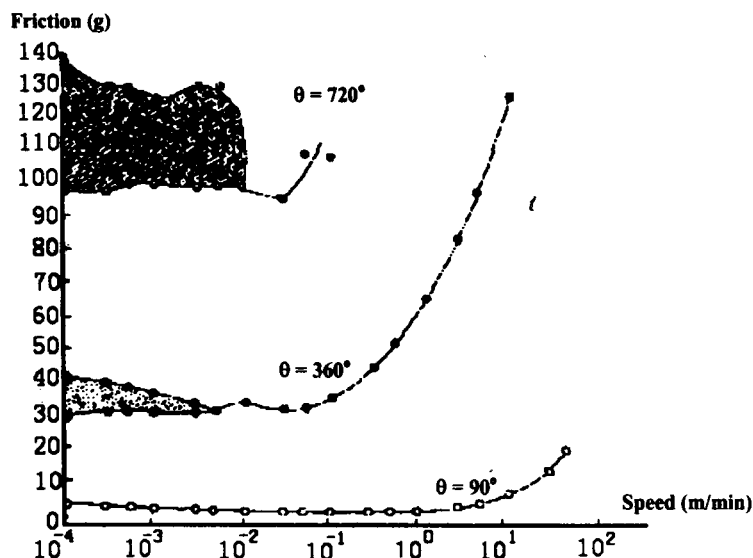


FIGURE 1. Effect of contact angle on friction with smooth pin [17].

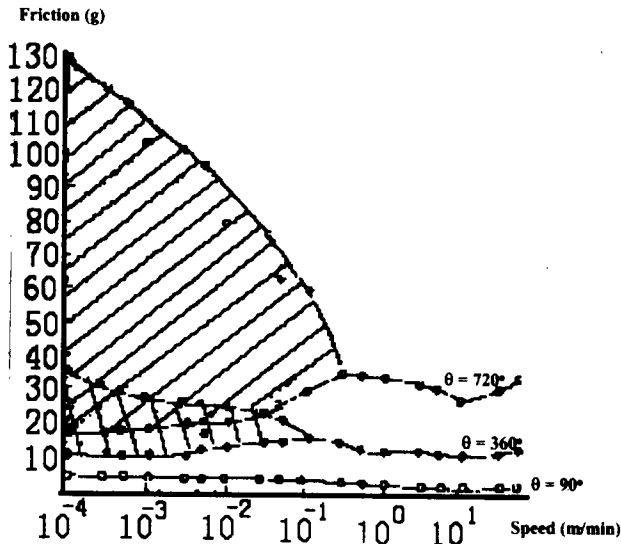


FIGURE 2. Effect of contact angle on friction with rough pin [17].

For instance, in Figure 1 where the surface of the guide is very smooth, $RMS = 4 \mu\text{in.} = 0.102 \mu\text{m}$, so that both the lubricant thickness and its variation are small. The yarn is virtually separated from the guide by the lubricant film, *i.e.*, the friction is hydrodynamic where frictional force in general increases in a nonlinear and drastic way with yarn speed and contact area (contact angle θ). But in Figure 2 with a very rough guide ($RMS = 60 \mu\text{in.} = 1.52 \mu\text{m}$), the direct contact between yarn and guide becomes inevitable and friction is largely of the semi-boundary or even boundary type. At the same speed, the frictional force in this case is low and also seems more or less proportional to the contact area (contact angle θ), as predicted in Equation 2, since there is much less room for change in lubricant thickness on a very rough surface. Therefore, Equation 2 is more applicable to semi-boundary or boundary friction.

Further, according to the theory of lubrication friction, if the friction type is hydrodynamic, the lubricant will stay and be pressed between the yarn and guide. The pressed lubricant film will inevitably deform along with the friction process, reducing its thickness. When the film thickness decreases to a certain degree, the surface of the yarn and guide will eventually contact each other. Consequently, the friction in a real case will often transfer from hydrodynamic to other types. Figure 1 is not consistent with Equation 2 because that equation becomes invalid when dealing with changes in lubricant thickness and hence the transformation of hydrodynamic to semi-boundary friction.

In this paper, we will analyze this transformation phenomenon and propose a new concept and calculation of the so-called effective length in a hydrodynamic fric-

tion process to quantitatively describe this friction transformation. Based on the effective length, we will develop a new theoretical scheme and conduct some parametric investigations.

Hydrodynamic Friction and Analysis of Friction Force

As a yarn slides through a cylindrical guide during hydrodynamic friction, the film thickness of the lubricant will, as previously mentioned, decrease along with the process, and the friction type will eventually transfer to semi-boundary friction. According to the theory of friction [6], this transformation point can be judged by a ratio $\lambda = \frac{h}{\sigma}$ of the film thickness h and surface roughness σ : when $\lambda > 3$, the process is considered hydrodynamic friction.

As the yarn passes through the cylindrical guide of radius R , as illustrated in Figure 3, the oil film stays between the yarn and the guide. A cross section of the yarn with diameter or thickness D and length $R \times \pi$ is illustrated in that figure.

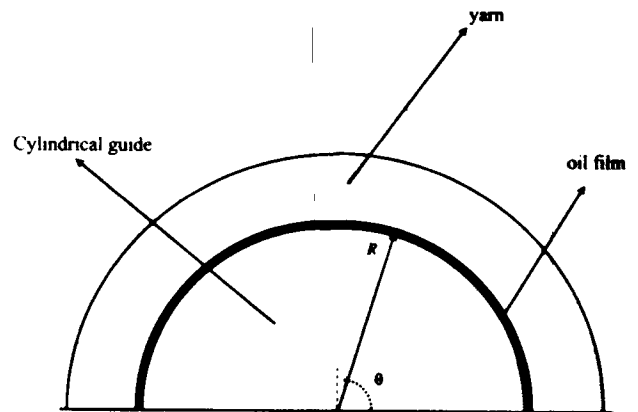


FIGURE 3. Yarn passing over a cylindrical guide.

To simplify the analysis, we have adopted the following assumptions: First, the lubricant oil is a Newtonian liquid. Second, the viscosity of the lubricant will remain constant within the frictional area; due to high speed, the contact time is too short to cause much change. Third, the pressure along a film thickness direction will be treated as constant for a small segment of yarn in Figure 4 at the instant of contact. Fourth, because of the diminutive contact time and constant pressure, the density of the lubricant will remain the same during the process.

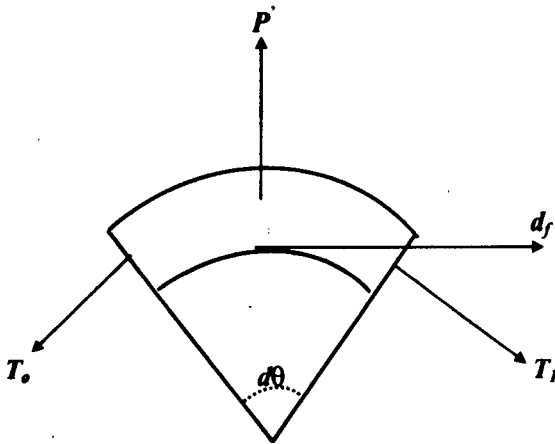


FIGURE 4. Force analysis.

Based on the illustration in Figure 4 of the force analysis on an arbitrary yarn element, Equation 3 can be derived as

$$T_1 \cos\left(\frac{d\theta}{2}\right) = T_0 \cos\left(\frac{d\theta}{2}\right) + df \quad (3)$$

where $d\theta$ is the contact angle of the yarn element, df is the frictional force acting on the element, and T_0 and T_1 are the initial yarn tension and the tension after the friction. The pressure on the lubricant film can be described by

$$P = -P' = T_1 \sin\left(\frac{d\theta}{2}\right) + T_0 \sin\left(\frac{d\theta}{2}\right) - \rho d\theta V^2 \quad (4)$$

where V (m/min) is the tangential velocity of the yarn, largely a constant, P' and P are the action and reaction forces (cN) between the film and the yarn, ρ is the linear density of the yarn, and R is the radius of the cylindrical guide. Substituting Equation 3 into 4 yields

$$P = 2T_0 \sin\left(\frac{d\theta}{2}\right) + df \tan\left(\frac{d\theta}{2}\right) - \rho d\theta V^2 \quad (5)$$

If the value of $d\theta$ is very small and we neglect the infinitely small term of the higher order, we obtain a simpler result:

$$P = T_0 d\theta - \rho d\theta V^2 \quad (6)$$

In Equation 6, since change in the second part in the right-hand side can be treated as negligible, the pressure P is mainly related to the initial tension of the yarn element T_0 , which as a whole increases in the yarn due to gradually induced friction as the yarn moves around the guide, increasing the pressure P . This in turn will

reduce the film thickness. This ever-decreasing thickness of the film will result in a changing frictional coefficient and hence the frictional nature during the whole process.

Changing Film Thickness

The system of yarn passing over the cylindrical guide could be considered as an extremely thin journal-bearing system because the ratio of yarn length to its width is large [6]. For such an infinitesimal journal-bearing model, the shear stress in the direction of the circle and the extrusive effectiveness of the fluid can be neglected. Consequently, the thickness of the film will not change. A constant film thickness is governed by Equation 2, which can be derived using the infinitesimal journal-bearing model [6] when the eccentricity is set to zero. Thus, it is clear that neglecting the shear stress and the extrusive effectiveness of the lubricant cannot generate a theory that can explain the contradiction between the experiment in Figure 2 and the theoretical prediction by Equation 2.

The moving track of the yarn element can be shown by changes in film thickness during the friction process because the yarn in fact slides forward on the surface of the film. The compound velocity of the yarn can be represented by both radial and tangential velocities, but it is the tangential velocity that causes the frictional force.

The radial velocity in fact represents the deformation rate of lubricant thickness due to pressure from the yarn, and the decrement of thickness is equal to the radial displacement of the yarn element. By definition, the radial velocity can be expressed as the derivative of the film thickness versus time t :

$$V_h = \frac{dh}{dt} \quad (7)$$

where dh is the thickness variation of the film.

According to the four earlier assumptions, the contact shape between the yarn element and the guide can be thought of as a rectangle. The relationship between the film thickness and the yarn pressure is thus derived as [6]

$$\frac{P}{L} = -\beta \frac{\eta D^3}{h^3} \frac{dh}{dt} \quad (8)$$

where L is the length of the yarn element in the direction of motion, D is the contacting width of the yarn element, which is equal to $0.087d$ (the yarn diameter) according to reference 19, h is the thickness of the film, η is the lubricant viscosity, and β is the so-called leaking coefficient (determined by the ratio of D to L , see Table I [6]). Combining Equations 7 and 8, we have

TABLE I. Relation between β and $\frac{D}{L}$ [6].

$\frac{D}{L}$	1	5/6	2/3	1/2	2/5	1/3	1/4	1/5	1/10	0
β	0.421	0.498	0.580	0.633	0.748	0.790	0.845	0.874	0.937	1

$$V_h = \frac{Ph^3}{\beta\eta LD^3} \quad (9)$$

$$\Delta t = \frac{\Delta T}{100} \quad (14)$$

From Equations 6 and 9, we can conclude that the radial velocity of the yarn element and hence the film thickness is mainly related to the initial tension of the yarn T_0 .

In hydrodynamic friction, the frictional force is formed by shear stress in the lubricant. Therefore, the frictional force in the yarn element is

$$df = \eta \frac{d_A V}{h} \quad (10)$$

where $d_A = R d\theta D$ is the contact area between the yarn element and the film.

If the whole frictional region is hydrodynamic friction, the total frictional force F and the equivalent frictional coefficient μ of differential element should be

$$F = \int_0^\theta \frac{\eta V R D}{h} d\theta \quad (11)$$

and

$$\mu = \frac{df}{P} = \frac{R\eta DV d\theta}{hP} \quad (12)$$

Calculation and Discussion

According to the scheme presented in Figure 3, the contact angle between the yarn and the guide is π . To facilitate the numerical calculation, the length of the yarn element can be chosen as $L = 10D$, where D is the contacting width of the yarn. The whole semi-circular section can then be divided into n parts:

$$n = \text{int} \left(\frac{\pi R}{L} \right) = \text{int} \left(\frac{\pi R}{10D} \right) \quad (13)$$

Then, from the entrance point of the yarn, an arbitrary part can be designated as i , and the last part n represents the exit point of the yarn. The entire passing time is by definition $\Delta T = \frac{L}{V}$. To minimize the calculating error, this time ΔT can be further divided into 100 elements of Δt , i.e.,

The reduction of lubricant thickness during Δt is then calculated as

$$\Delta h = V_h \Delta t = \frac{Ph^3}{100V\beta\eta D^3} \quad (15)$$

and the increment of the frictional force Δf during Δt follows from

$$\Delta f = \eta \frac{d_A V}{h} = \frac{10V\eta D^2}{h} \quad (16)$$

In yarn part i , the initial tension is $T_{i,0}$ and the initial thickness of the film is $h_{i,0}$. If the passing time of yarn part i is time j , the initial tension of the yarn should be $T_{i,j}$ ($j = 1, 2, 3, \dots, 100$) and the initial thickness of the oil film should be $h_{i,j}$. During the time from j to $j + 1$, the increment of the frictional force is $\Delta f_{i,j}$ and the decrement of the film thickness is $\Delta h_{i,j}$, so it is obvious that

$$T_{i,j+1} = T_{i,j} + \Delta f_{i,j} \quad (17)$$

and

$$h_{i,j+1} = h_{i,j} + \Delta h_{i,j} \quad (18)$$

When the yarn travels from part i to part $i + 1$, the initial tension of the yarn element and the initial thickness of the oil film in part $i + 1$ should be

$$T_{i+1,0} = T_{i,0} + \sum_{j=1}^{100} \Delta f_{i,j} \quad (19)$$

and

$$h_{i+1,0} = h_{i,0} + \sum_{j=1}^{100} \Delta h_{i,j} \quad (20)$$

Using the data in Table II and with the entire friction region divided into 100 parts from the initial point to the exit point, the ratio of the film thickness at the arbitrary part h_i to the initial film thickness h_0 can be used to describe the relationship of the lubricant thickness versus

the relative location over the entire frictional region, as shown in Figure 5.

TABLE II. Data used for calculations.

Property	Symbol	Value	Unit
Initial tension	T_0	10	g
Velocity	V	25	m/s
Viscosity	η	44.1	cp
Yarn diameter	d	0.1	mm
Guide diameter	R	64	mm
Initial film thickness	h_0	5	μm
Contact angle	θ	π	-
Guide roughness	σ	0.102	μm

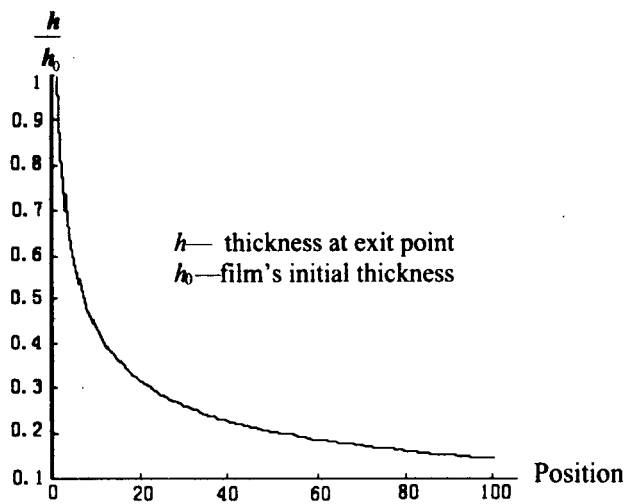


FIGURE 5. Film thickness versus location over the entire friction region (in relative scale).

The film thickness initially decreases very rapidly in Figure 5, and the change rate of the film thickness decreases during the friction process. When the value of film thickness is near that of guide surface roughness, the yarn will inevitably contact the guide and hydrodynamic friction will turn into semi-boundary friction. For instance, if the guide surface roughness σ is $0.102 \mu\text{m}$ ($4 \mu\text{in.}$), according to the criterion mentioned earlier, the critical condition for the semi-boundary is $h < 3\sigma = 0.306 \mu\text{m}$. From Figure 5, the thickness of the exit point is about $h_0 \times 0.2 = 1 \mu\text{m} > 3\sigma$, so the entire friction region is hydrodynamic friction.

Also, this reduction in lubricant thickness will lead to an increasing climb in frictional force based on Equation 10. Consequently, the frictional force of the entire friction region will not be linear or proportional to the contact area or the contact angle θ , as predicted in Figure 6.

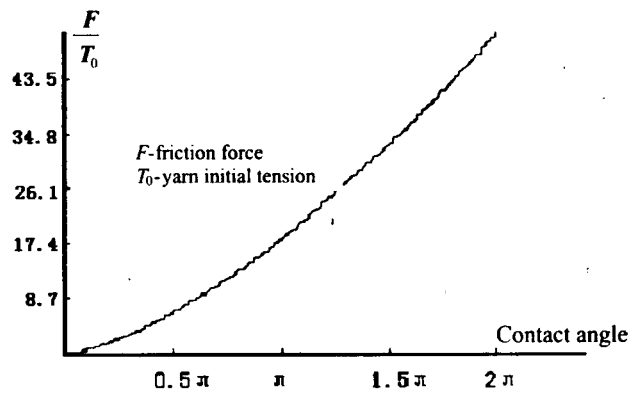


FIGURE 6. Relative friction force versus contact angle.

This nonlinearity of the ascending frictional force is consistent with that in Figure 1 at a contact area of low roughness. Therefore, our theory can be used to describe the hydrodynamic friction process and may explain the contradictions in the experimental results in Figures 1 and 2 and thus compensate for the limitation of Equation 2.

If the tangential velocity of the yarn increases, the time the yarn acts on the film will obviously decrease. At the same time, the compression rate of the lubricant thickness will abate, as indicated in Equation 15, so the film thickness in the exit point will increase with increasing yarn velocity. The calculated curve of lubricant thickness versus velocity is presented in Figure 7. On the other hand, according to Equation 10, the frictional force will increase with escalating yarn velocity, as shown in Figure 8. These two competing factors do not, however, cancel each other, because according to Figure 7, the changing rate of yarn velocity is higher than that of the film thickness in the given range. Thus, the frictional force should increase with escalating yarn velocity according to Equation 10. This is again consistent with the experimental findings [4, 5, 8].

If the roughness of the guide surface σ is such that the ratio of lubricant thickness to roughness, $\lambda = h/\sigma$, will at some point before the exit become smaller than 3 because of reducing h , the hydrodynamic friction will then transform into the semi-boundary state. In this case, the duration or effective length of the hydrodynamic frictional process can be represented by a dimensionless value ψ , defined as

$$\Psi = \frac{L^1}{L^0} \quad (21)$$

where L^1 represents the actual length of hydrodynamic friction, and L^0 is the total length of the entire friction region. A greater ψ value thus corresponds to a higher

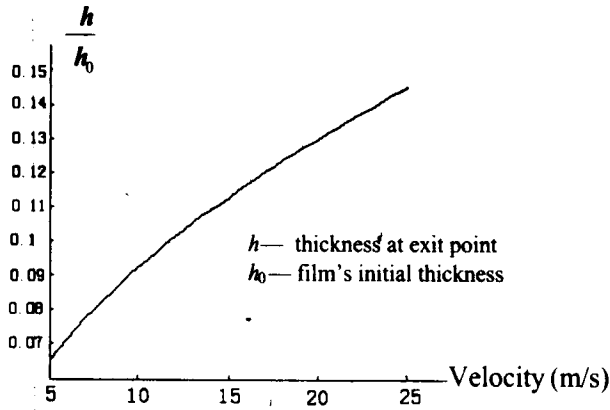


FIGURE 7. Relative film thickness at the exit versus yarn velocity.

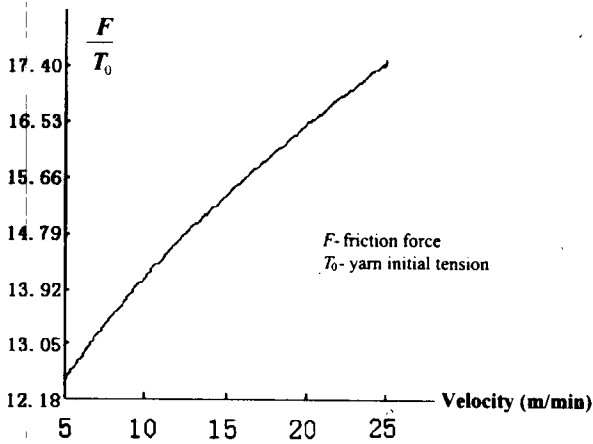


FIGURE 8. Relative friction force versus yarn velocity.

proportion of the hydrodynamic friction process. The relationship between ψ and the surface roughness guide is shown in Figure 9, based on the aforementioned transformation criterion.

From Figure 9, we see that the length of hydrodynamic friction is to a great extent determined by guide surface roughness. If the roughness is beyond $1.5 \mu\text{m}$, the effective length diminishes, *i.e.*, there will be no hydrodynamic friction process. This result is in good agreement with the experiments in Figures 1 and 2: roughness = $0.102 \mu\text{m}$ and $1.524 \mu\text{m}$, respectively.

Thus, this roughness effect must be considered when studying the frictional behavior between the cylinder guide and yarn, since the friction mechanism in this case is entirely determined by guide roughness. In fact, to avoid a hydrodynamic process characterized by great frictional force, the surface of the yarn guide on the winding machine is made relatively rough. Once the hydrodynamic friction ceases due to great roughness, the

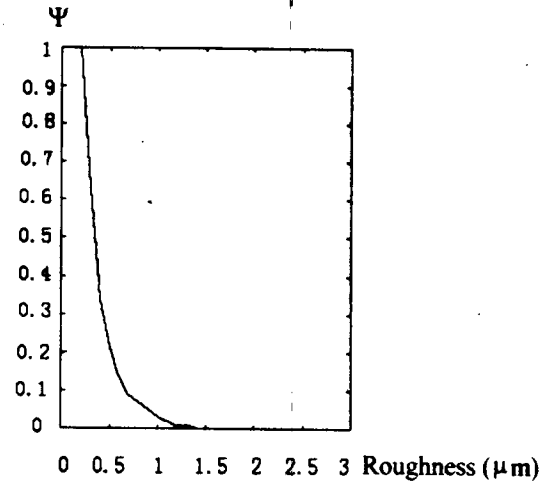


FIGURE 9. Hydrodynamic effective friction length versus guide roughness.

friction will convert to a semi-boundary state with entirely different behavior.

Conclusions

In hydrodynamic friction, the extrusive effect on the film cannot be neglected: the pressure exerted by the yarn on the lubricant film decreases the film thickness and increases the frictional force significantly. This is consistent with the experimental results in Figure 1.

Hydrodynamic friction is characterized by very high frictional force due to the shearing resistance from the lubricant. Increasing such factors as yarn speed V , lubricant viscosity η , yarn diameter d , and tension T will encourage hydrodynamic friction or high friction.

If all other factors are given, the nature of a frictional process is entirely determined by the roughness of the guide surface σ . If roughness decreases, hydrodynamic friction will become semi-boundary or boundary friction due to the gradual elimination of the lubricant between yarn and guide. The effective length of the hydrodynamic friction ψ is a useful index for specifying the relative duration of hydrodynamic friction.

The nature of the friction or the magnitude of the frictional force or the equivalent frictional coefficient between yarn and guide changes during the entire friction process. Therefore the Euler equation is not able to explain such a frictional phenomenon.

Literature Cited

1. Ajayi, J. O., and Elder, H. M., Effects of Surface Geometry on Fabric Friction, *J. Test. Eval.* **25**, 182 (1997).

2. Ajayi, J. O., and Elder, H. M., Effects of Finishing Treatments on Fabric Friction, *J. Test. Eval.* **23**, 55 (1995).
3. Ajayi, J. O., and Elder, H. M., Comparative Studies of Yarn and Fabric Friction, *J. Test. Eval.* **22**, 463 (1994).
4. Baird, M. E., and Mieszkis, K. W., Friction Properties of Nylon Yarn and Their Relation to the Function of Textile Guides, *J. Textile Inst.* **46**, 101 (1955).
5. Bowden, F. P., and Young, J. E., Friction of Diamond, Graphite, and Carbon and the Influence of Surface Films, *Proc. R. Soc.* **A208**, 444 (1951).
6. Cameron, A., "Basic Lubrication Theory," ch. 9, Ellis Horwood, NY, 1976.
7. Fort, T. Jr., Boundary Friction of Textile Yarns, *Textile Res. J.* **31**, 1007 (1961).
8. Hansen, W. W., and Taber, D., Hydrodynamic Factors in the Friction of Fibers and Yarns, *Textile Res. J.* **27**, 300 (1957).
9. Howell, H. G., The General Case of Friction of String Round a Cylinder, *J. Textile Inst.* **44**, T359 (1953).
10. Howell, H. G., The Friction of a Fiber and Round a Cylinder and Its Dependence upon Cylinder Radius, *J. Textile Inst.* **45**, T575 (1954).
11. Lincoln, B., The Frictional Properties of the Wool Fiber, *J. Textile Inst.* **45**, T92 (1954).
12. Lyne, X., The Dynamic Friction between Cellulose Acetate Yarn and a Cylindrical Metal, *J. Textile Inst.* **46**, 112 (1955).
13. Olsen, J. S., Friction Behavior of Textile Yarns, *Textile Res. J.* **39**, 31 (1969).
14. Ravandi, S. A. H., Toriumi, K., and Matsumoto, Y., Spectral Analysis of the Stick-slip Motion of Dynamic Friction in the Fabric Surface, *Textile Res. J.* **64**, 224 (1994).
15. Rubinstein, C., The Friction and Lubrication of Yarns, *J. Textile Inst.* **49**, 13 (1958).
16. Schick, M. J., Friction and Lubrication of Synthetic Fibers, Part I: Effect of Guide Surface Roughness and Speed on Fiber Friction, *Textile Res. J.* **43**, 103 (1973).
17. Schick, M. J., Friction and Lubrication of Synthetic Fibers, Part III: Effect of Guide Temperature, Loop Size, Pre-tension, Denier, and Moisture Regain on Fiber Friction, *Textile Res. J.* **43**, 254 (1973).
18. Schick, M. J., Friction and Lubrication of Synthetic Fibers, Part V: Effect of Fiber Luster, Guide Material, Charge, and Critical Surface Tension of Fibers on Fiber Friction, *Textile Res. J.* **44**, 758 (1974).
19. Schlatter, C., and Demas, H. J., Friction Studies on Caprolan Filament Yarn, *Textile Res. J.* **32**, 87 (1962).
20. Schlatter, C., and Onley, R. A., Concerning the Mechanisms of Fiber and Yarn Lubrication, *Textile Res. J.* **29**, 200 (1959).
21. Taylor, P. M., and Pollet, D. M., The Low-force Frictional Characteristics of Fabrics against Engineering Surfaces, *J. Textile Inst.* **91**, 1 (2000).

Manuscript received September 24, 2002; accepted April 4, 2003.